Titel/Title: Indirect fluorescence-based in situ geometry measurement for laser chemical machining

Autor*innen/Author(s): Andreas Fischer, Merlin Mikulewitsch, Dirk Stöbener

Veröffentlichungsversion/Published version: Postprint

Publikationsform/Type of publication: Artikel/Aufsatz

Zusätzliche Informationen/Additional information:

Accepted for publication in CIRP Annals.
Corresponding author:
Andreas Fischer, University of Bremen, Bremen Institute for Metrology, Automation and Quality Science (BIMAQ), Bremen, Germany
andreas.fischer@bimaq.de

Indirect fluorescence-based in situ geometry measurement for laser chemical machining

Andreas Fischer[a,*], Merlin Mikulewitsch[a], Dirk Stöbener[a,b]

[a] University of Bremen, Bremen Institute for Metrology, Automation and Quality Science (BIMAQ), Linzer Str. 13, 28359 Bremen, Germany
[b] MAPEX Center for Materials and Processes, Bibliothekstr. 1, 28359 Bremen, Germany

Submitted by Prof. Ekkard Brinksmeier (1), University of Bremen, Germany

A B S T R A C T

Optical geometry measurements of submerged workpiece surfaces in the chaotic fluid environment of laser chemical machining (LCM) are challenging, because the produced cavities feature high aspect ratios and surface gradients. To avoid reflection-based artefacts at high gradients, molecules are added to the acid, whose fluorescence is detected with a confocal setup. The model-based signal processing enables the indirect measurement of the micro-geometry even in acid layers with mm to cm thickness and is capable to cope with process-inherent bubbles. As a result, the geometry measurement is shown to be applicable for the LCM process at surface gradients up to 84°.

Keywords:
Optical
Photochemical machining
Indirect geometry measurement

* Corresponding author.
E-mail address: andreas.fischer@bimaq.de (A. Fischer).

1. Introduction

The LCM manufacturing process uses an electrolytic liquid in combination with a localized energy input by laser light to achieve a material removal that enables the production of microstructures with high surface gradients, small edge radii and high aspect ratios on the immersed workpiece [1]. Compared to processes such as micro-milling or laser ablation, there are advantages such as lower costs and tool wear as well as reduced thermal stress on the edge zone of the component [2]. However, since the workpiece is immersed in a liquid, the in situ geometry measurement required for quality control is difficult to achieve with conventional tactile methods. The in situ conditions of the LCM process also impose high challenges for optical measuring methods. Interferometric methods such as white light interferometry [3,4] are not applicable because the measurement deviations caused by thermal gradients and refractive index fluctuations are too large [3]. Confocal microscopy, which is also frequently applied in other processes, is prone to the high surface angles and curvatures typically produced with the LCM process [4,5], so that commercial sensors based on this principle are also not suitable for LCM. However, the variant of confocal fluorescence microscopy is promising for an LCM application, since it does not capture the light reflected by the sample, but the light emitted by a fluorescent liquid covering it. The sample surface as a common boundary layer between liquid and sample is characterized by a decrease of the fluorescence signal during vertical scanning of the confocal volume through the liquid (perpendicular to the liquid surface). This method of indirect geometry measurement has already been successfully used by Liu et al. on metallic microspheres with high curvatures by coating the sample surface with a thin fluorescent film $< 100\,\mathrm{nm}$ [5]. They were able to detect light even at angles $> 75°$ from the surface normal with a lateral resolution comparable to conventional confocal microscopy without generation of the otherwise known 'bat wing' artifacts. Takaya et al. successfully used the method to measure a cutting tool edge in situ, while being covered by a thin ($< 113\,\mu\mathrm{m}$) layer of fluorescent cutting fluid, to determine tool wear [6].

In the LCM process, however, thicker liquid layers $> 1\,\mathrm{mm}$ are present. As a result, the fluorescence signal shows dependencies on the fluorophore concentration, the liquid depth and the refractive index. The resulting influence on the measured surface coordinates requires a model-based evaluation [7]. To what extent the thicker fluid layer affects the detection of high surface angles and curvatures, and what impact disturbances caused by fluid contamination (e.g. gas bubbles generated by the process) have, is not yet known and is of great importance for the application of the measurement approach in the LCM process.

Therefore, this article aims to assess the applicability of the indirect geometry measurement in the LCM process with respect to the influences of surface angle and fluid contamination. For this purpose, the principle and the evaluation of the indirect geometry measurement are presented in Section 2, as well as the necessary evaluation modifications. Section 3 describes the setup and sample geometry used for the influence investigations and the results obtained. Section 4 completes the paper with conclusions and an outlook on pending work.

2. Indirect geometry measurement method

2.1. Principle, signal model and evaluation

The principle of the indirect geometry measurement is based on the detection of light emitted by a fluid, in which the specimen is

submerged, instead of light scattered or reflected on the specimen surface [8]. By employing a technique capable of axial light sectioning, the detected fluorescence signal $S(z)$ can be limited to a small volume around the focal plane of the objective. This is achieved by confocal microscopy (cf. Fig. 1), where a pinhole, that is confocal to the objective plane, attenuates light originating far from the objective focal plane.

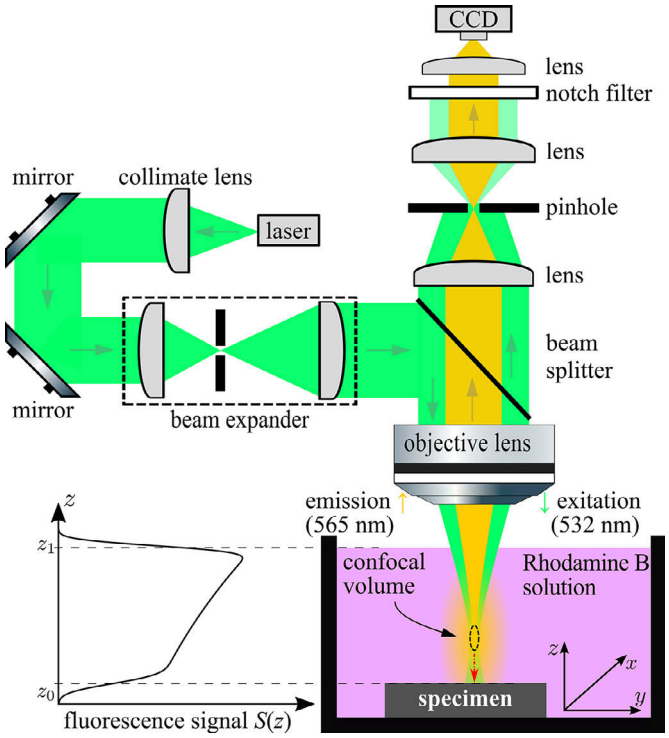

Fig. 1. Diagram of the indirect measurement setup based on confocal microscopy. The specimen surface position z_0 is obtained from the fluorescence signal $S(z)$ (bottom left) via model-based evaluation. The numerical apertures of the fluorescence and excitation light beams are equal and are shown differently only for illustration purposes.

A signal is only detected when the so-called *confocal volume* intersects the fluorescent fluid. The light emitted in the intersection volume is then focused through the pinhole onto the detector. When the focal z-position exceeds the fluid boundaries z_0 (specimen surface) and z_1 (fluid surface), the detected fluorescence signal drops off. The specimen surface position z_0 can be inferred from the signal decrease at the fluid boundaries by using the confocal volume as a probe to scan vertically through the fluid (z-direction). By repeating this pointwise vertical scan in the x, y-plane, the surface geometry $z_0(x, y)$ is determined [7]. For thick fluid layers $> 100\,\mu$m, however, the determination of the position z_0 is not trivial, due to significant absorption along the optical path. For such applications, a model-based approach for the signal processing of the fluorescence signal $S(z)$ is required to achieve micrometer resolution [8].

The signal model is based on a confocal volume function $I(x, y, z)$. It describes the spatial distribution of the contributions of all infinitesimal volume elements to the totally detected fluorescence light power. The shape of the confocal volume is approximated by the 3-dimensional Gaussian function

$$I(x,y,z) = A \cdot \varepsilon \cdot \exp{-\frac{2}{w_0}\left(x^2+y^2+\frac{z^2}{\kappa^2}\right)}, \tag{1}$$

with a width of w_0 in x, y-direction and scaled by κ in z-direction. The fluorophore concentration is taken into account by the attenuation coefficient ε, and the excitation power as well as the fluorophore quantum yield by the parameter A. Since absorption is a non-negligible factor in thick fluid layers, the confocal volume function needs to be weighted by a depth (z) dependent attenuation term $\eta(z) = e^{\varepsilon(z-z_1)}$ according to the Lambert-Beer law of absorption [8]. The total detected fluorescence signal $S(z)$ at the position z is then obtained by integrating all weighted contributions to the signal over all three spatial dimensions [9]. Due to the simplifications towards the confocal volume shape, an analytical solution of the integral

$$\begin{aligned} S(z) &= \int_{z_0}^{z_1}\int_{-\infty}^{\infty}\int_{-\infty}^{\infty} \eta(\tilde{z})\cdot I(x,y,\tilde{z}-z)\,\mathrm{d}\tilde{x}\,\mathrm{d}\tilde{y}\,\mathrm{d}\tilde{z} \\ &= S_0\, e^{\varepsilon(z-z_1)}\left(\operatorname{erf}\left(\frac{z-z_0}{2\xi}+\varepsilon\xi\right)-\operatorname{erf}\left(\frac{z-z_1}{2\xi}+\varepsilon\xi\right)\right)+\text{const.} \end{aligned} \tag{2}$$

exists with $S_0 = (1/2)A\varepsilon w_0^2\xi\pi^{3/2}\exp(\xi^2\varepsilon^2)$ being the amplitude and $\xi = (\sqrt{2}/4)\kappa w_0$ being the confocal volume shape parameter. The parameters S_0, ξ, ε, the position z_1 (fluid surface) as well as the desired position z_0 (specimen surface) are obtained by using the model function $S(z)$ for a non-linear least-squares approximation of the measured data. Note that the scaling of the signal due to focusing through an interface is corrected according to [7].

2.2. Model extension for the LCM application

Besides the assumptions that underlie the current signal model, such as the disregard of fluorophore saturation and reabsorption or the simplified shape of the confocal volume, the assumptions made about the interactions of confocal volume and specimen surface are paramount for measurements at highly inclined surfaces occurring in the LCM process. Particularly notable are the discounted surface reflection and the assumption that the intersection between confocal volume and specimen surface is parallel to the x, y-plane, disregarding the surface inclination. These assumptions were found to be the cause of significant model uncertainties at high inclinations, necessitating an expansion of the current model. Based on measurements on highly inclined surfaces where the fluorescence signal was observed to deviate from the expected pattern, the signal model was heuristically extended by two additional terms. Including a second error function pair with a different shape parameter ξ and a further boundary position z_2 as well as an added Gaussian function with a width σ, weighted by the parameters K_1 and K_2 respectively, results in the modified model function

$$\begin{aligned} \widehat{S}(z) = S_0\, e^{\epsilon(z-z_1)}&\left[\operatorname{erf}\left(\frac{z-z_0}{2\Xi}+\epsilon\Xi\right)-\operatorname{erf}\left(\frac{z-z_1}{2\Xi}+\epsilon\Xi\right)+K_1\cdot\right. \\ &\left.\left(\operatorname{erf}\left(\frac{z-z_2}{2\xi}+\epsilon\xi\right)-\operatorname{erf}\left(\frac{z-z_1}{2\xi}+\epsilon\xi\right)\right)\right]+K_2 e^{-\frac{(z-z_2)^2}{2\sigma^2}}+\text{const.} \end{aligned} \tag{3}$$

which was found to be superior to the unmodified model in terms of model uncertainties.

3. Experimental investigations regarding LCM application

To demonstrate the potential of the indirect measurement technique for the LCM process application, measurements on strongly inclined surfaces and in a process fluid, contaminated with high gas bubble densities, were carried out and analyzed with the extended signal model.

3.1. Experimental setup and used specimen

The used confocal fluorescence microscope setup is shown schematically in Fig. 1. A green diode laser (25 mW, $\lambda = 532$ nm) is widened by a Kepler beam expander and diverted by a beam splitter to the objective lens (NA = 0.42, WD = 20 mm). The objective focuses this excitation light into the fluid, consisting of a dilute aqueous solution of Rhodamine B, surrounding the submerged specimen. The fluid container is positioned with a 3-axis linear stage to scan the focus position through the fluid. Both the fluorescent light emitted by the fluid ($\lambda = 565$ nm) and the scattered excitation light ($\lambda = 532$ nm) are recaptured by the objective lens and returned through the beam splitter. They are focused onto a pinhole (diameter: 5 μm) confocal to the objective lens, which attenuates the light coming far from the focal plane and thus produces the confocal effect. Behind the pinhole, the excitation light is filtered from the fluorescence light by a notch filter (center wavelength: 532 nm). The fluorescence intensity signal

is lastly measured by a detector, in this case a charge-coupled device (CCD) sensor, averaged over all 1280 × 960 pixels.

The specimen used for high surface inclination measurements consists of a brass block with six inclined surfaces, as shown in Fig. 2. The inclined surfaces start with 1 cm offset to the specimens back side at the height of the flat top surface with a width of 1 cm respectively and an inclination of 35°, 45°, 55°, 65°, 75° and 85° (rounded to integer) respectively.

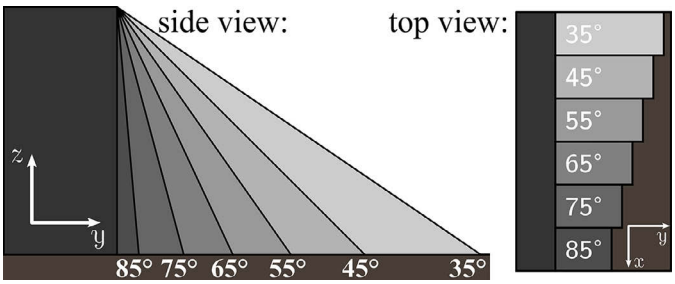

Fig. 2. Diagram of the brass specimen with six surface inclinations.

Reference measurements of the specimen using conventional laser scanning confocal microscopy yielded a mean Rz roughness of $(6.3 \pm 1.7)\,\mu$m. As expected, the conventional technique suffers from artifacts at the highest inclination of 85° and requires several acquisition steps with different integration times, if more than one inclination is included in the field of view.

3.2. Results

3.2.1. Measurement at high surface inclination

For the assessment of the inclination influence on the measurements, the surface positions of three different inclinations were measured on the specimen shown in Fig. 2. The specimen surface is submerged in a fluid layer (1 mm – 7.5 mm), depending on the position on the inclined surface. To avoid submerging the objective lens, the measured fluid thickness was limited to 7.5 mm. However, employing a submersible objective lens or one with a greater working distance enables measuring thicker fluid layers. The fluorescence signals for five points along a line in y-direction on the 65° inclined surface of the submerged specimen (cf. Fig. 2) are shown in Fig. 3, with the approximated model functions resulting from a non-linear least squares fit using Eq. (3) (black lines). The calculated specimen surface positions z_0 are shown as black circles. The measurement was performed on the specimen surface inclinations 35°, 65° and 85°.

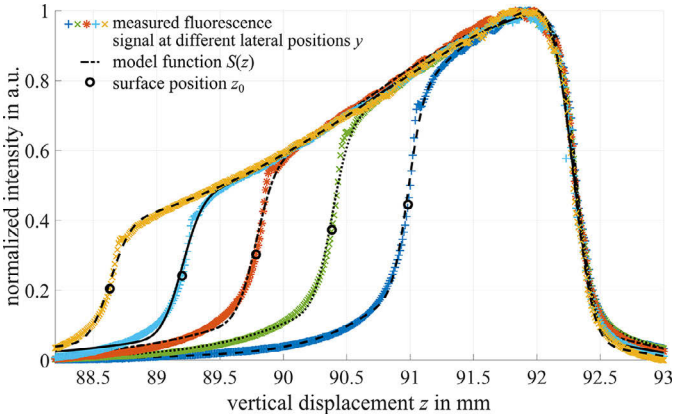

Fig. 3. Measured fluorescence signal with model fit for an excerpt of five y-positions on the 65° inclined surface of the specimen from Fig. 2.

The modified model function $\hat{S}(z)$ is thereby shown to successfully enable the surface position measurement. The positions z_0 for one line in y-direction on each surface are shown in Fig. 4a) respectively.

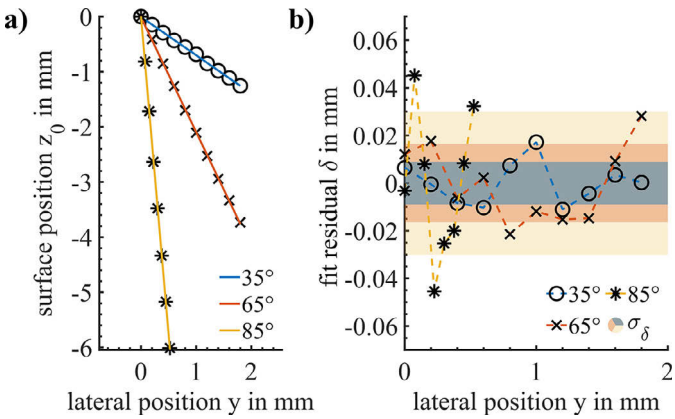

Fig. 4. Surface position measurements: a) Results for different nominal surface inclinations with their respective linear fits; b) Fit residuals δ of the linear fits and their standard deviations σ_δ for the different surface inclinations (colored with their respective inclination).

The plane surfaces of the specimen were approximated with linear fits, shown as solid lines. As a result, the measurement is shown to be suitable even on highly inclined surfaces up to 84.3° In contrast to reference measurements of the 85° surface with conventional confocal microscopy, no artifacts were observed with the indirect measurement.

The deviation of 0.7° from the nominal angle of the specimen surface can be explained by manufacturing tolerances and a small tilt of the specimen relative to the optical axis. The fit residuals δ of the three measurements are shown in Fig. 4b) respectively. The standard deviation σ_δ of each fit residual is depicted as a shaded area. It is discernible that the standard deviation increases with the surface angle, with a standard deviation of the fit residual of 30.1 μm for the 85° inclination. However, the same effect can be observed in the reference measurements performed with conventional confocal microscopy. Here, the standard deviation of the fit residuals of the 85° inclination deviates only up to 10 % from the standard deviation of the indirect measurement shown in Fig. 4, depending on which exact location on the specimen surface is evaluated.

The fit residual is assumed to be a superposition of the surface topography and the measurement uncertainty. Since the natural variations of the topography (i.e. roughness, see Sect. 2.2) on the inclined surfaces are assumed to be uniform over the inclined surfaces in a first approximation, the uncertainty contribution prevails. Consequently, the measurement uncertainty is found to increase with the surface inclination both for the indirect as well as the conventional measurement. This increase is mainly caused by the higher fluid layer thickness above the measurement points towards more strongly inclined surfaces, which is known to increase the uncertainty [8]. Another cause is the naturally larger distribution of different vertical surface positions in the lateral extent of the confocal volume due to the inclined intersection between confocal volume and surface.

In order to reveal the full potential for steep surface gradients and more complex surface geometries, shadowing needs to be taken into account in future studies, which means that a part of the light path to and from the confocal volume is obstructed by a steep surface.

3.2.2. Influence of fluid contaminants

In order to assess the influence of fluid contaminants, the process environment of laser chemical machining was emulated by adding highly concentrated phosphoric acid (5 molar) to the fluorescent fluid. This led to a process-analog chemical production of hydrogen bubbles on the surface of a non-passivating sample placed in the fluid. As a contrast, a self-passivating sample was also added, which produced no additional gas bubbles, see Fig. 5a). The fluorescence signals resulting from measurements in this emulated process environment are shown in Fig. 5 with b) low bubble density in the optical path at position x_1 and c) high bubble density at position x_2. The low bubble density over the self-passivating material, where no chemical

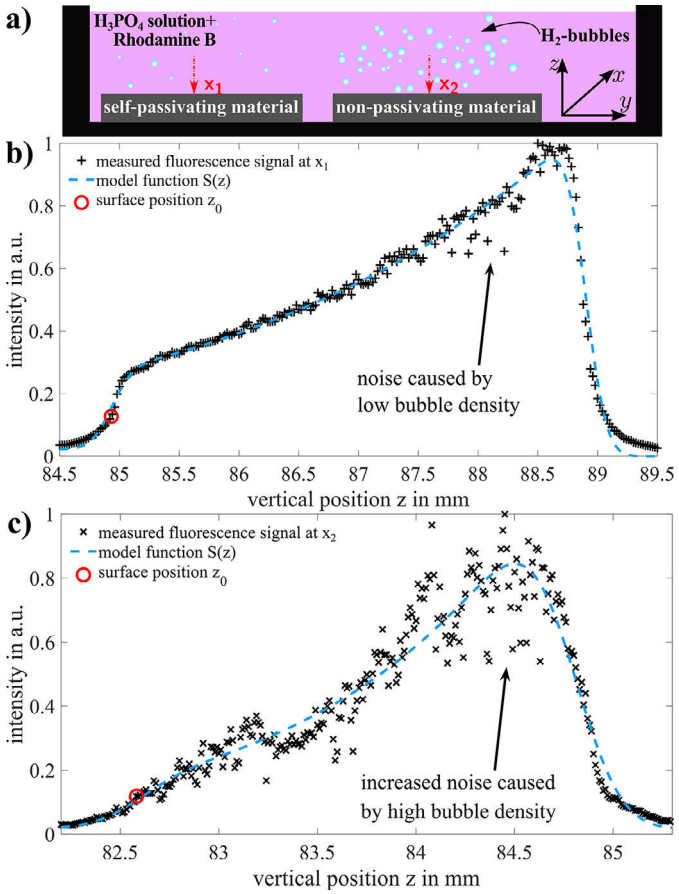

Fig. 5. Gas bubble influence on the fluorescence signal: a) Setup to generate gas bubbles via chemical reactions; b) and c) Fluorescence signals at positions x_1 and x_2 with the bubble density dependent noise.

reaction takes place, is caused by diffusion of bubbles in the fluid container. The measurements show that the bubble density is directly responsible for the noise level of the fluorescence signal, especially near the fluid surface, where rising bubbles disrupt the smooth surface boundary and cause refraction of the fluorescence light to occur. However, as a result of the model-based signal evaluation, the determination of the surface position z_0 is possible even under the influence of increased signal noise (cf. Fig. 5c).

4. Conclusions

A model-based indirect geometry measurement is realized for fluid layers $>$ 1 mm and is shown to be applicable at different surface gradients up to 84° while still offering μm resolution. In contrast to the reference measurement using conventional confocal techniques, the indirect measurement with an extended signal model exhibits no artifacts at steep slopes while at the same time offering a comparable deviation from the nominal geometry. The indirect measurement of the micro-geometry is also shown to work even in conditions similar to the LCM process environment such as acid layers $>$ 1 mm and process-inherent gas bubbles in the optical path. Despite an increased signal noise, the measurement of the surface geometry using the model-based evaluation is still feasible. As a result, the indirect measurement approach with μm-resolution is shown to be suitable for the in situ application in thick fluid environments like the LCM process, where process-oriented measurements are as yet not possible. Due to similarly challenging process conditions (thick fluid environment) and complex workpiece geometries (highly inclined surfaces), further potential in situ applications of the indirect geometry measurement are electro-chemical and electrical discharge machining.

Acknowledgements

This work was funded by the German Research Foundation in the Collaborative Research Center 747. The authors wish to thank Prof. Dr.-Ing. habil. Dr.-Ing. E. h. E. Brinksmeier for his sponsorship of this paper.

References

[1] Messaoudi H, Mikulewitsch M, Brand D, von Freyberg A, Fischer A (2019) Removal Behavior and Output Quality for Laser Chemical Machining of Tool Steels. *Manufacturing Review* 6:13.
[2] Ahmed N, Darwish S, Alahmari AM (2016) Laser Ablation and Laser-Hybrid Ablation Processes: A Review. *Materials and Manufacturing Processes* 31(9):1121–1142.
[3] Gerhard C, Vollertsen F (2010) Limits for Interferometric Measurements on Rough Surfaces in Streaming Inhomogeneous Media. *Product Engineering Research and Development* 4(2–3):141–146.
[4] Hansen H, Carneiro K, Haitjema H, De Chiffre L (2006) Dimensional Micro and Nano Metrology. *CIRP Annals* 55:721–743.
[5] Liu J, Liu C, Tan J, Yang B, Wilson T (2016) Super-Aperture Metrology: Overcoming a Fundamental Limit in Imaging Smooth Highly Curved Surfaces. *Journal of Microscopy* 261(3):300–306.
[6] Takaya Y, Maruno K, Michihata M, Mizutani Y (2016) Measurement of a Tool Wear Profile Using Confocal Fluorescence Microscopy of the Cutting Fluid Layer. *CIRP Annals* 65(1):467–470.
[7] Mikulewitsch M, Auerswald M, von Freyberg A, Fischer A (2018) Geometry Measurement of Submerged Metallic Micro-Parts Using Confocal Fluorescence Microscopy. *Nanomanufacturing and Metrology* 1(3):171–179.
[8] Mikulewitsch M, von Freyberg A, Fischer A (2019) Confocal Fluorescence Microscopy for Geometry Parameter Measurements of Submerged Micro-Structures. *Optics Letters* 44(5):1237–1240.
[9] Malzer W, Kanngießer B (2005) A Model for the Confocal Volume of 3D Micro X-ray Fluorescence Spectrometer. *Spectrochimica Acta Part B: Atomic Spectroscopy* 60 (9–10):1334–1341.